

Comparison of Staphopain A (ScpA) and B (SspB) precursor activation mechanisms reveals unique secretion kinetics of proSspB (Staphopain B), and a different interaction with its cognate Staphostatin, SspC

Nicholas Nickerson,^{1†} Jessica Ip,^{1†} Daniel T. Passos² and Martin J. McGavin^{2*}

¹Department of Laboratory Medicine and Pathobiology, University of Toronto, Toronto, Ontario, Canada, M4N 3M5.

²Department of Microbiology and Immunology, University of Western Ontario, London, Ontario, Canada, N6A 5C1.

Summary

The *scpAB* and *sspABC* operons of *Staphylococcus aureus* encode Staphopain cysteine proteases ScpA and SspB, and their respective Staphostatins ScpB and SspC, which are thought to protect against premature activation of Staphopain precursors during protein export. However, we found that the proSspB precursor was secreted and activated without detriment to *S. aureus* in the absence of SspC function. Our data indicate that this is feasible due to a restricted substrate specificity of mature SspB, a stable precursor structure and slow secretion kinetics. In contrast, mature ScpA had a broad substrate specificity, such that it was prone to autolytic degradation, but also was uniquely able to degrade elastin fibres. Modelling of proScpA relative to the proSspB structure identified several differences, which appear to optimize proScpA for autocatalytic activation, whereas proSspB is optimized for stability, and cannot initiate autocatalytic activation. Consequently, recombinant proSspB remained stable and unprocessed when retained in the cytoplasm of *Escherichia coli*, whereas proScpA initiated rapid autocatalytic activation, leading to capture of an activation intermediate by ScpB. We conclude that the status of *sspBC* in *S. aureus*, as paralogues of the ancestral *scpAB* genes, facilitated a different activa-

tion mechanism, a stable proSspB isoform and modified Staphostatin function.

Introduction

Staphylococcus aureus causes infections in virtually every tissue and organ system of the body (Archer, 1998; Lowy, 1998), with adhesion proteins of the MSCRAMM family promoting efficient colonization of tissues where the underlying ECM is exposed (Patti *et al.*, 1994; Patti and Hook, 1994), followed by rapid invasion of the surrounding tissues, leading to bacteremia and metastatic infections (Fowler *et al.*, 2007). A secreted serine protease (SspA; V8 protease) may promote invasion by degrading fibronectin-binding MSCRAMMs (McGavin *et al.*, 1997), and is part of the staphylococcal proteolytic cascade (SPC), which is initiated by rapid autocatalytic activation of the metalloprotease Aureolysin (Nickerson *et al.*, 2007). Aureolysin (Aur) then activates SspA encoded by the staphylococcal serine protease operon *sspABC* (Nickerson *et al.*, 2007; 2008), and the SspA glutamyl endopeptidase in turn activates a precursor of the SspB cysteine protease, which is also encoded by the operon (Rice *et al.*, 2001; Massimi *et al.*, 2002). SspB is one of two cysteine proteases, Staphopain A (ScpA) and Staphopain B (SspB), produced by *S. aureus*. The less virulent coagulase-negative Staphylococci (CNS) represented by *S. epidermidis* have orthologues of Staphopain *scpA*, Aureolysin (*aur*) and the *sspA* serine protease. However, the *sspA* locus is monocistronic in the CNS group, with the exception of *S. warneri*, which also has an *sspABC* operon (Yokoi *et al.*, 2001; Golonka *et al.*, 2004; Dubin *et al.*, 2007).

In addition to being members of the papain family, Staphopains A and B are expressed in respective operons *scpAB* and *sspABC*, where the Staphopain genes *scpA* and *sspB* are followed by genes encoding Staphostatins ScpB and SspC, which inhibit the respective Staphopains by forming a 1:1 protein complex (Filipek *et al.*, 2003; 2005; Rzychon *et al.*, 2003; Wladyka *et al.*, 2005). The Staphopains are also both secreted as inactive precursors, proScpA and proSspB, from which the N-terminal

Accepted 11 November, 2009. *For correspondence. E-mail mmcgavin@uwo.ca; Tel. (+1) 519 850 2458; Fax (+1) 519 661 3499.
†Denotes an equal contribution to this work.

Table 1. Microbial strains used or constructed in this study.

Strain	Description (source)
<i>S. aureus</i>	
RN6390	<i>sigB</i> deficient lab strain with elevated protease production (Peng <i>et al.</i> , 1988); identical to strain 8325-4
SP6391	RN6390 with a non-polar <i>sspA::erm</i> insertion within the <i>sspABC</i> operon (Rice <i>et al.</i> , 2001)
6390_Pspac:: <i>sspABC</i>	RN6390 with the <i>sspABC</i> operon disrupted by integration of Pspac:: <i>sspA</i>
RN6390_Pspac:: <i>sspC</i>	RN6390 with the <i>sspABC</i> operon disrupted by insertion of pMUT_BC
RN4220	Restriction deficient host strain (Novick, 1991)
Newman	Historical ST8 clinical isolate (Baba <i>et al.</i> , 2008)
USA300	ST8 community-acquired MRSA (Li <i>et al.</i> , 2009)
USA400/MW2	ST1 community-acquired MRSA (Baba <i>et al.</i> , 2002)
WBG10049	ST30spa19 community-acquired MRSA (Robinson <i>et al.</i> , 2005)
M1015	ST30spa43 historical pandemic strain (Robinson <i>et al.</i> , 2005)
M809	ST30spa43 historical pandemic strain (Robinson <i>et al.</i> , 2005)
ATCC25923	'Seattle 1945'; single locus MLST variant of ST30 (American Type Culture Collection)
BK12003	ST30 MSSA; spa type 19 (Barry Kreiswirth)
L516	ST30spa33 strain from osteomyelitis patient; Winnipeg 1994 (Lindsay Nicolle)
MN8	ST30spa33 historical TSST strain (Blomster-Hautamaa and Schlievert, 1988)
L528	ST30spa33 bacteremia isolate; Winnipeg, 1994 (Lindsay Nicolle)
<i>E. coli</i>	
DH5 α	Host strain for construction of recombinant plasmids
XL-1Blue	Host strain for site-directed mutagenesis of plasmid DNA
DH10B	Host strain for arabinose-inducible expression vector
M15pREP	Host strain for IPTG-inducible expression vector (Qiagen)

propeptides must be removed to produce an active protease. For proSspB, this occurs when the SspA glutamyl endopeptidase processes at QE↓₂₂₀DQVQ to release mature SspB (Massimi *et al.*, 2002), comprising the end-point of the SPC pathway. However, the activation mechanism and substrate specificity of ScpA have not been defined.

The Staphostatins are reported to protect Staphylococci from premature activation of Staphopain precursors during protein export, based on an *sspC::tet* derivative of *S. aureus* 8325-4 showing a severe phenotype characterized by slow growth, altered cellular morphology, and a profound defect in production of cell-surface and secreted proteins (Shaw *et al.*, 2005). These observations served as the basis for a model of Statin function encompassing cysteine proteases of both *S. aureus* and *S. pyogenes* (Potempa *et al.*, 2005), but were contrary to our unpublished data, where in anticipation of a deleterious phenotype, we constructed an ectopic expression mutant of *sspC*, but did not observe any deleterious phenotype. Because the *sspBC* genes likely evolved in *S. aureus* as paralogues of the ancestral *scpAB* locus, and paralogues by definition have new or modified functions compared with their ancestral genes, we undertook to resolve this discrepant finding by conducting a detailed comparison of the activation mechanism, stability and substrate specificity of Staphopain A, and its interaction with cognate Staphostatin A (ScpB), in relation to Staphopain B (SspB) and Staphostatin B (SspC). We find that the two Staphopains are polar opposites in terms of their activation mechanisms, and

their interaction with and requirement for cognate Staphostatins, and conclude that the SPC pathway incorporates multiple safeguards to minimize premature activation of proSspB, including control at the level of protein trafficking to minimize the interaction between proSspB and proSspA, and a precursor structure that is incapable of autocatalytic activation.

Results

Loss of Staphostatin SspC is not detrimental

Details on bacterial strains and plasmids used in this study are provided in Tables 1–3. Ectopic expression of Staphostatin SspC was achieved by integration of pMUT_BC (Table 2) within the *sspABC* operon. The 540 bp fragment cloned in pMUT_BC spans the 3' end of *sspB* and first 51 nucleotides of *sspC* (Table 2), such that integration into the *sspABC* operon maintained the integrity of *sspAB*, but placed *sspC* under transcriptional control of the inducible Pspac promoter of the parent pMUTIN4 vector (Vagner *et al.*, 1998). In RN6390_Pspac::*sspC*, a Western blot of cell-lysate confirmed that SspC was expressed only when induced with IPTG (Fig. 1A). RN6390 and isogenic Pspac::*sspC* derivative grown without IPTG both secreted abundant proSspB at 5 h of growth (Fig. 1B), which was then converted to mature SspB. As there was no obvious phenotype associated with this mutation, we next constructed a Δ *sspC::erm* deletion. After 18 h in BHI broth (Fig. 2), the Δ *sspC::erm* and Pspac::*sspC* mutants secreted a spec-

Table 2. Plasmids used or constructed in this study.

Plasmid	Comments
pUC18	<i>E. coli</i> cloning vector
pUscpAB	scpAB expression cassette amplified from genomic DNA of <i>S. aureus</i> RN6390 with primers <i>scpA_F1</i> and <i>scpB_R1</i> , and cloned into the BamHI and EcoRI sites of pUC18
pUscpA _(C>A) B	Cys ₂₃₈ >Ala active site substitution of ScpA, constructed by PCR mutagenesis of pUC_scpAB with mutagenic primers MP_scpA1 and MP_scpA2
pUC_erm::BC	pUC18 containing an <i>erm</i> :: <i>sspBC</i> transcriptional fusion, amplified from genomic DNA of <i>S. aureus</i> SP6391 with primers <i>sspA_F1</i> and <i>sspBC_R1</i>
pQE30	<i>E. coli</i> vector for IPTG-inducible expression of N-terminal 6His-tagged proteins (Qiagen)
p6H_proScpA _(C>A)	Cys ₂₃₈ >Ala variant of <i>scpA</i> , cloned at the BamHI and PstI sites of pQE30. The cloned product was amplified by PCR with pUscpA _(C>A) B plasmid template, using primers <i>scpA_F2</i> and <i>scpA_R1</i>
p6H_proSspB	proSspB cloned in pQE30, by PCR amplification with primers <i>sspB_F1</i> and <i>sspB_R1</i>
pBAD24	<i>E. coli</i> vector for arabinose-inducible expression of recombinant protein (Guzman <i>et al.</i> , 1995)
pBAD_ScpAB _{6H}	pBAD24 containing <i>scpAB</i> cassette that was amplified by PCR with primers <i>scpA_F3</i> (BspHI), and <i>scpB_6HR1</i> (PstI) incorporating a C-terminal 6×His tag, then cloned into the NcoI and PstI sites of pBAD24
pBAD_SspBC _{6H}	pBAD24 containing <i>sspBC</i> cassette that was amplified by PCR with primers <i>sspB_F2</i> (BspH 1) and <i>sspC_6HR1</i> (Pst1), then cloned into the NcoI and PstI sites of pBAD24
pBAD_SspC _{6H}	<i>sspC</i> cloned in pBAD-Topo TA (Invitrogen), with a C-terminal 6×His tag (Massimi <i>et al.</i> , 2002)
pRN5548a	Promoterless derivative of <i>S. aureus</i> plasmid pRN5548, which contains the multiple cloning site of pUC18 (Novick, 1991)
pRscpAB	scpAB expression cassette from pUscpAB excised with BamHI and EcoRI, and cloned into the complementary sites of pRN5548
pRscpA _(C>A) B	Cys>Ala active site variant of the <i>scpAB</i> operon, excised from pUscpA _(C>A) B with BamHI and EcoRI and cloned into the complementary sites of pRN5548
pPQ126	Gram-positive plasmid vector containing the E194ts temperature-sensitive replication origin (Luchansky <i>et al.</i> , 1989)
pMUTIN4	Suicide vector containing the IPTG-inducible <i>Pspac</i> promoter, for construction of ectopic expression mutants in Gram-positive bacteria (Vagner <i>et al.</i> , 1998)
pMUT_BC	pMUTIN4 containing a 540 bp PCR product spanning the 3' end of <i>sspB</i> and first 51 nucleotides of <i>sspC</i> , amplified with primers <i>sspB_F3</i> (HindIII) and <i>sspC_R2</i> (BamHI)
pMUTΔlacZ	A <i>lacZ</i> deletion derivative of pMUTIN4 created by inverse PCR with primers Mut_F1 and Mut_R1 to incorporate a <i>Stul</i> site, then re-ligated after digestion with <i>Stul</i>
pMUT_E194ts	A HincII fragment containing the E194ts temperature-sensitive replication origin of pPQ126, cloned into the unique <i>Stul</i> site of pMUTΔlacZ
pMUT_sspA	pMUT_E194ts with the 5' end of the <i>sspA</i> gene placed under transcriptional control of the <i>Pspac</i> promoter; a 346 bp insert beginning with the ribosome binding site of <i>sspA</i> was amplified by PCR with <i>sspA_F1</i> and <i>sspA_R1</i> , and cloned into the HindIII and BamHI sites of pMUT_E194ts, placing the 5'-end of the <i>sspA</i> gene under transcriptional control of the <i>Pspac</i> promoter

trum of proteins similar to RN6390, with the exception of what appeared to be reduced SspA and SspB protein. Diminished production of mature SspB was confirmed by Western blot. As the mutants were cultured with erythromycin, which could affect the efficiency of translation of polycistronic mRNAs, we repeated the experiment with cultures grown for 8 h in TSB as in Fig. 1, but without antibiotics. The impact on production of SspA, which is needed to activate proSspB, was less evident under these conditions, although Western blotting revealed minor differences in the abundance of mature SspA and the isoforms in its step-wise activation. Importantly, the Δ *sspC*::*erm* strain demonstrated effective production of mature SspB. Therefore, although we cannot state conclusively whether minor differences in the amount of SspA and SspB production are due to loss of SspC function, or alternately due to destabilization of the truncated *sspAB* transcript, we conclude that loss of *sspC* function had no major adverse effect on growth, viability, protein secretion or function of the SPC pathway. We therefore undertook to determine why there was no detrimental phenotype.

Slow secretion of preproSspB

We observed two isoforms of proSspB in cell lysate of RN6390, of which the smaller comigrated with proSspB purified from an *sspA*::*erm* derivative of RN6390 (Massimi *et al.*, 2002), and was sensitive to Proteinase K-treatment of a cell suspension, while the larger was not affected (Fig. 3A). The proSspB isoform was released when cells were converted to spheroplasts, but the larger isoform was not (Fig. 3B), supporting its identity as preproSspB with a non-cleaved signal peptide. To determine if retention was inherent to the protein, we took advantage of *sspBC* being fused to *ermB* in strain SP6391, due to the non-polar *sspA*::*erm* mutation (Rice *et al.*, 2001), allowing us to amplify an expression cassette comprised of *ermB* followed by the 3' end of *sspA* and intact *sspBC* genes. When this cassette was cloned into pUC18, *Escherichia coli* transformed with the plasmid produced the same two isoforms (Fig. 3C). When the cells were treated with polymyxin, proSspB partitioned to the periplasmic fraction, which also contained some preproSspB, but most of the preproSspB was retained by the spheroplasts, indicating

Table 3. Oligonucleotides used for PCR and site-directed mutagenesis.

Primer	Sequence ^a	Co-ordinates (5'/3')
scpA_F1 ^b	Bam HI CTACGCTTCTTTCAAATCG	-223/-204
scpB_R1	Eco RI TTATGACTTATGCTTAATGAAAGTC	2385/2361
MP_scpA1	CTCAAGGTAACAATGGTTGGcgCGCAGGCTATACGATGTCT	692/732
MP_scpA2	AGACATCGTATAGCCTGCcgC CCA ACCATTGTACCTTGAG	732/692
scpA_F2	Bam HI GAGAGCAATTC AAAT ATCAAAGC	76/98
scpA_R1	Pst I TTATGACTTATGCTTAATGAAAGTC	2385/2361
scpA_F3	Bsp HI ACGCTGAGAGCAATTC AAAT ATCAAAGC	931/959
scpB_6HR1	Pst I CAATGGTGATGGTGATGATG TGACTTATGCTTAA TGAAAGTCATTCTAGG	2382/2353
sspA_F1 ^c	Pst I CCTACTGGTACATTTATTGCTTCC	645/668
sspB_F1	Bam HI GATTCACACTCTAAACAGC	1554/1572
sspB_F2	Bsp HI at GCCGATTCACACTCTAAACAGCTAG	1551/1575
sspB_F3	Hind III GCAGGATTCAGTATGGCAGC	2175/2194
sspB_F4	CCCTAACAAACCCAGATGAACC	1262/1282
sspB_R1	Pst I TTAGTAACCTATCATTGAACCATACC	2627/2602
sspBC_R1	Pst I TGATATTAAGTCACTTGGCGTCC	3219/3198
sspC_6HR1	Pst I CAATGGTGATGGTGATGATG TACTAAGCGCTCAT AAACGATTGGTCCG	2991/2965
sspC_R2	Bam HI TGTGAGTTTGGTTGTGTCG	2715/2697
sspC_R3	TTATACTAAGCGCTCATAAACG	2994/2973
Mut_F1 ^d	Stu I TCCAGTTCAACATCAGCCGC	3227/3246
Mut_F2	GGTGTTGGCATAATGTGTG	250/267
Mut_R1	Stu I TAACGCCAGGGTTTTCCCAG	427/408
Mut_R2	Same as pMUT_R1, but without 5'-StuI site	
sspA_F1	Hind III TGGAGGTTTTAGATGAAAGG	341/361
sspA_R1	Bam HI CTTTACCTACAACCTACACCGGAAG	687/664

a. Lower case nucleotides in the mutagenic primers indicate altered codons; 5' additions to the PCR primers used for cloning are indicated in bold, with restriction sites in subscript text, and 6 × His tag segments underlined. The ATG translation initiation codon embedded in the *sspA*_F1 primer is underlined.

b. The nucleotide co-ordinates for the *scpA* and *scpB* primers are numbered with +1 corresponding to the first nucleotide in the ATG initiation codon of the *scpA* gene SAOUHSC_02127, and numbered contiguously to the end of *scpB* (SAOUHSC_02129) from the *S. aureus* NCTC 8325 genome sequence (AF309515). Nucleotides 5' of the initiation codon are numbered with negative integers.

c. Co-ordinates of primers within the *sspABC* operon are derived from GenBank AF309515.

d. Co-ordinates of the MutF1 and MutR1 primers used for inverse PCR of pMUTIN4 are derived from the similar pMUTIN2 sequence (AF072806).

that retention is inherent to the protein. There was no evidence of mature SspB in the periplasm (data not shown), confirming as described previously (Massimi *et al.*, 2002; Rice *et al.*, 2001), that proSspB is stable in the absence of SspA.

We next conducted a temporal analysis of proSspB secretion, relative to SspA, and α -hemolysin (Hla), which is an important secreted virulence factor of *S. aureus* (Bubeck Wardenburg *et al.* 2007; Wardenburg and Schneewind, 2008). At mid-exponential phase (3 h), there were no proSspA isoforms in total cell lysate of RN6390, but proSspA was present and processed in the culture supernatant (Fig. 4A). Conversely, preproSspB was detected in the 3 h cell lysate (Fig. 4B), which had only a trace of proSspB, and the culture supernatant also had only a trace of proSspB, relative to the more abundant proSspA. At 6 h, there was again abundant cell-associated preproSspB, but no significant proSspA isoforms, while the supernatant had abundant proSspB, as well as proSspA and its activation intermediates. In the same samples, Hla was abundant in the supernatant (4C), and there was a small amount of cell-associated Hla, but

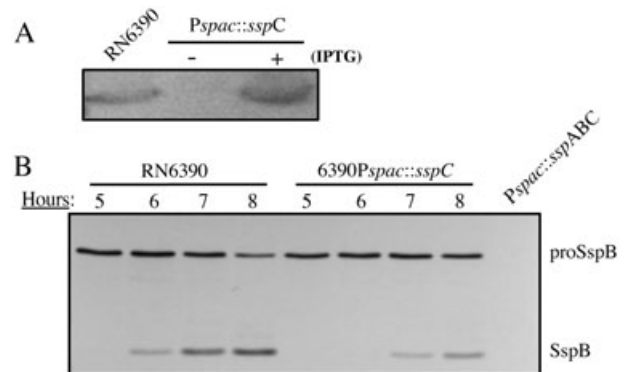


Fig. 1. Western blot of total cell lysate (A) or secreted proteins (B) produced by *S. aureus* RN6390 or isogenic *Pspac::sspC* derivative. For (A), cells were grown in the absence or presence of 1 mM IPTG for induction of SspC expression from the *Pspac::sspC* promoter fusion, and the Western blot was probed with affinity-purified antibodies specific for SspC. For (B), cultures were grown in TSB and samples of cell free culture supernatant were prepared at the indicated time points. Blots were developed with affinity-purified antibodies specific for SspC (A) or proSspB (B). The amount of protein loaded was equivalent to 1.0 OD₆₀₀ unit of cell lysate (A), or 0.02 OD₆₀₀ unit of culture supernatant (B). Strain RN6390 *Pspac::sspABC* that is deficient in expression of the *sspABC* operon was used as a negative control for (B).

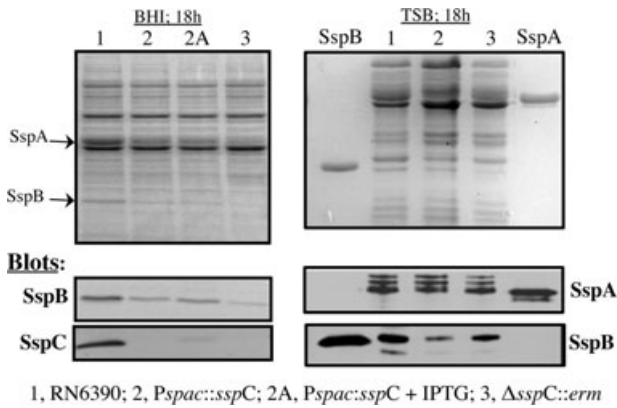


Fig. 2. SDS-PAGE of secreted proteins produced by *S. aureus* RN6390 and isogenic derivatives, grown for 18 h in BHI (left panels) or 8 h in TSB (right panels). For the mutant strains, BHI medium contained $10 \mu\text{g ml}^{-1}$ erythromycin, while TSB did not contain antibiotic. The upper left and right panels show profiles of secreted proteins resolved by SDS-PAGE and protein stain. The bottom panels represent Western blots for detection of SspA or SspB in culture supernatant, or SspC in total cell lysate. Protein loading was equivalent to 1.0 OD₆₀₀ unit of TCA precipitated protein for protein profiles; 0.05 OD₆₀₀ unit for detection of SspA and SspB in culture supernatant, or 2.0 OD₆₀₀ units of total cell lysate in Western blot assay for detection of SspC. Purified protein standards consisted of 1 μg of purified mature SspA or SspB for protein stain, and 200 ng of SspA or SspB for Western blot.

no indication of a preHla isoform. Therefore, cellular retention is unique to preproSspB.

Differential stabilities of proStaphopains

We next evaluated the stability of proSspB relative to the Staphopain A precursor, proScpA. For this purpose, *E. coli* was transformed with plasmids p6H_proScpA_(C>A)

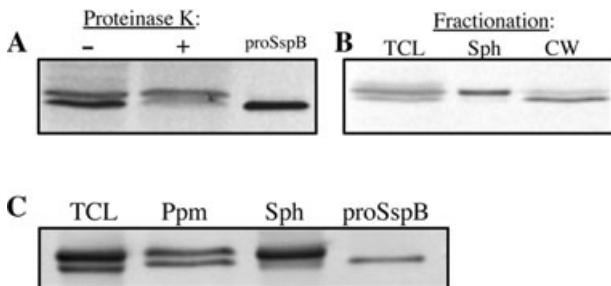


Fig. 3. Western blot for detection of cell-associated SspB isoforms in *S. aureus* (A and B) or *E. coli* cells transformed with pUCerm::BC (C), developed with antibodies specific for proSspB. In (A), a *S. aureus* cell suspension (1×10^{10} cfu ml⁻¹) was pre-treated with or without Proteinase K prior to preparation of the total cell lysate. For (B), the cell suspension was treated with lysostaphin to prepare a total cell lysate, or with lysostaphin in the presence of 17% sucrose, followed by centrifugation to separate the spheroplast pellet (Sph) from the soluble cell wall protein fraction (CW). For (C), the *E. coli* suspension was sonicated to obtain total cell lysate (TCL), or treated with Polymyxin followed by centrifugation to separate the Spheroplast (Sph) and soluble periplasmic (Ppm) fractions. In each panel, the amount of protein loaded was equivalent to 1.0 OD₆₀₀ unit of culture. (A) and (C) also included 100 ng of purified proSspB as a standard.

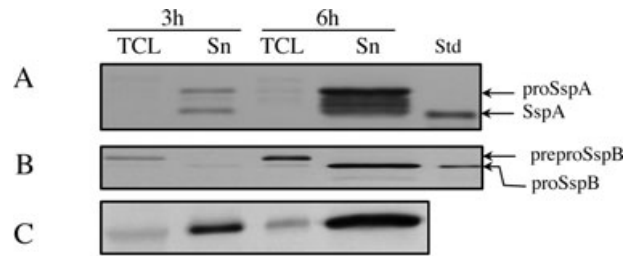


Fig. 4. Western blot for detection of SspA (A), SspB (B) or Hla (C) isoforms in total cell lysate (TCL) and culture supernatant (Sn) of *S. aureus* RN6390 after 3 and 6 h of growth as indicated. At the indicated time points, aliquots of the cultures were removed and rapidly mixed with an equal volume of ice cold 50 mM sodium azide and 200 μM CCCP, prior to centrifugation to obtain the cell pellet and cell free supernatant fractions. A sample volume equivalent to 0.05 OD₆₀₀ unit was applied to all lanes, with exception of the 3 h culture supernatant (0.2 OD₆₀₀). The Standard lane (Std) contained 50 ng of either mature SspA (A) or proSspB (B) as indicated.

or p6H_proSspB, derived from pQE30 (Table 2). In these vectors, the signal sequence of the Staphopain is replaced by a 6 \times His tag to ensure cytoplasmic retention, and allow purification of the precursors by metal affinity chromatography (MAC), while proScpA only was modified by a Cys>Ala active site substitution, to render it inactive. After induction of expression with IPTG, 6H-proSspB was prominent in the cell lysate, and was recovered in good yield after MAC of the soluble fraction of cell lysate (Fig. 5). Comparatively, 6H-proScpA_(C>A) was less abundant in cell lysate, and was recovered in low yield by MAC, where it copurified with more abundant 60 and 20 kDa polypeptides, identified by trypsin digestion and

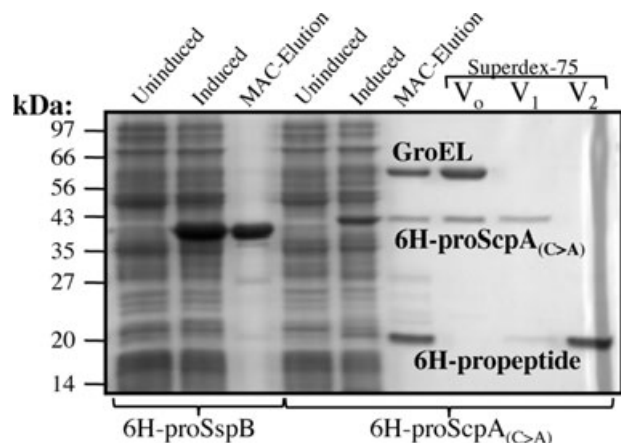


Fig. 5. SDS-PAGE and protein stain of total cell lysate from *E. coli* cells transformed with either p6H_proSspB or p6H_proScpA_(C>A). Protein in the soluble fraction of cell lysate was subjected to MAC, where 6H-proSspB or 6H-proScpA_(C>A) were eluted from the matrix with an imidazole gradient (MAC-Elution). Eluted 6H-proScpA_(C>A) and copurifying proteins were further fractionated on Superdex 75, which resolved three peaks designated V₀ (void volume), V₁ and V₂ as indicated. Individual proteins in the 6H-proScpA_(C>A) are as labelled on the figure.

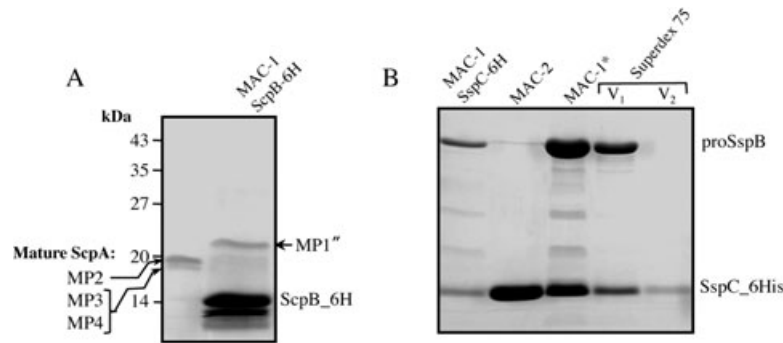


Fig. 6. SDS-PAGE and protein stain showing (A) 2 µg of mature ScpA purified from *S. aureus*, and protein eluted on MAC (MAC-1 ScpB_{6H}) of lysate from *E. coli* transformed with pBAD_{scpAB}_{6H}. (B) shows protein eluted from MAC of lysate from *E. coli* cells transformed with pBAD_{sspBC}_{6H}, which eluted as two peaks designated MAC-1 and MAC-2. The MAC-1 fractions were concentrated (MAC-1*) and applied to Superdex 75, where two peaks, V₁ and V₂, were resolved. Specific proteins are labelled on the left or right margins of each figure, and the identities of the MP1'', MP2, MP3 and MP4 isoforms of mature ScpA protease are specified in the schematic diagram of proScpA (Fig. 7A).

mass spectrometry as the cytoplasmic chaperone GroEL, and the N-terminal propeptide of 6H-proScpA_(C>A) respectively. When passed through a Superdex-75 column, proScpA_(C>A) and GroEL eluted as a complex in the void volume (V₀), followed by a peak V₁ that contained 6H-proScpA only, and peak V₂ comprised of the N-terminal propeptide. Therefore, in the cytoplasm of *E. coli*, 6H-proScpA(C>A) formed a complex with GroEL, and was processed to release its N-terminal propeptide.

Staphopain–Staphostatin interactions

Processing of 6H-proScpA_(C>A) in *E. coli* to release an N-terminal propeptide domain (Fig. 5) should also have produced mature ScpA, which if not for the Cys>Ala substitution, would be an active protease. Therefore, we expected that coexpression of native proScpA with Staphostatin ScpB would lead to capture of mature ScpA in complex with ScpB. We first identified the native N-terminus of mature ScpA, purified from culture supernatant of *S. aureus* strain Pspac::sspABC (Table 1), transformed with pRscpAB (Table 2). The sspABC operon is not expressed in this strain (Fig. 1B), due to insertion of pMUT_{sspA} after the ribosome binding site of sspA, allowing ScpA to be purified free from other proteases. Purified ScpA had three isoforms of mature protease (MP) (Fig. 6A), which as defined in a schematic representation of proScpA (Fig. 7A), consisted of the larger and more abundant MP2 (₂₁₀SNNYT), and two smaller overlapping MP3 and MP4 isoforms, of which MP3 matched the N-terminus of Staphopain from *S. aureus* strain V8 (Hofmann *et al.*, 1993).

To determine if these isoforms could be captured in complex with ScpB in the cytoplasm of *E. coli*, pBAD_{scpAB}_{6H} was used to promote arabinose-inducible expression of scpAB, where scpB is modified to incorpo-

rate a C-terminal 6His tag, and scpA has its signal peptide deleted, but retains a native active site. After induction with arabinose, MAC of protein in the soluble fraction of cell lysate yielded a single peak MAC-1 (Fig. 6A), comprised of abundant ScpB_{6H}, and a less abundant protein that was larger than mature ScpA. The N-terminus of this protein corresponded to a transient MP1''-isoform of MP (Fig. 7A), processed at LK_{↓197}QK, several amino acids prior to the N-terminus of the major MP2 isoform, indicating that an early activation intermediate was captured in complex with ScpB. Using a similarly designed pBAD_{sspBC}_{6H} vector (Fig. 6B), two peaks were eluted from the metal affinity matrix. The major MAC-2 peak consisted almost exclusively of SspC_{6H}, while the faster eluting and minor MAC-1 contained 40 and 14 kDa proteins, corresponding to proSspB and SspC_{6H} respectively. When the MAC-1 peak was concentrated (MAC-1*), and passed through a Superdex 75 column, proSspB and most of SspC_{6H} coeluted as a complex V₁, followed by a minor peak V₂ containing SspC_{6H} only. There was no evidence of mature SspB, confirming that proSspB was not processed in the cytoplasm of *E. coli*, but unexpectedly, some of the total proSspB was recovered in complex with Staphostatin SspC.

Rapid autocatalytic activation of proScpA

Using the pRscpAB vector to promote expression and secretion of recombinant proScpA in RN6390 Pspac::sspABC, we identified processing events that are mapped on a diagram of proScpA (Fig. 7A), and the resulting polypeptides are labelled in the profile of secreted proteins (Fig. 7B and C), where a polypeptide triplet ranging from 17 to 20 kDa was evident after 6 h of growth (Fig. 7B and inset). The N-terminus of the 17 kDa component matched with proScpA after processing by signal pepti-

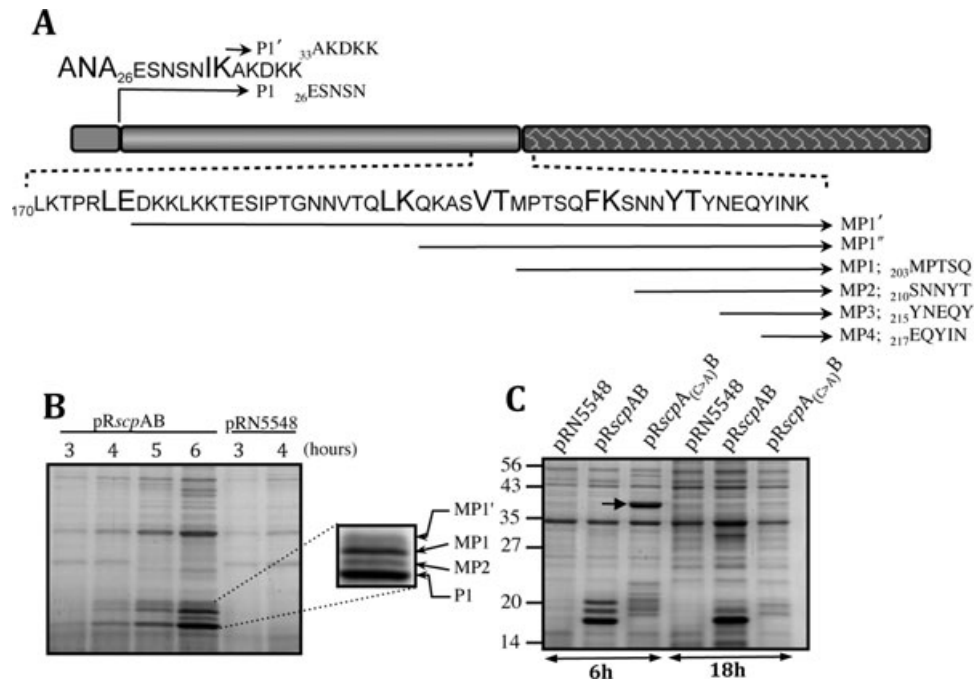


Fig. 7. A. Schematic representation of preproScpA showing the signal peptide (dark grey; amino acids 1–25), N-terminal propeptide and Staphopain A domains. The amino acid sequence of the signal peptidase processing site and N-terminus of proScpA is shown above the diagram, and an expansion of the amino acid sequence spanning the juncture of the N-terminal propeptide and mature ScpA domains is represented below the sequence. Processing sites are shown in large font, and the N-terminal segment of each resulting isoform is indicated by an arrowed line, labelled according to the identity of each isoform in the profile of secreted proteins, shown in (B).

B. SDS-PAGE and protein stain of secreted proteins produced by *S. aureus* RN6390 *Pspac::sspABC* transformed with pRscpAB or blank pRN5548 vector. TCA precipitated protein, equivalent to 1.0 OD₆₀₀ unit of culture supernatant harvested at the indicated times, was applied to each lane. The inset provides an enlargement of processing intermediates, showing the identity of the P1, MP1 and MP2 polypeptides as determined by N-terminal sequencing for P1, MP1 and MP2, or for MP1' deduced from mass values of propeptide fragments as shown in Fig. 8, and defined in Table 4 and the text of the Results section.

C. SDS-PAGE comparing secreted proteins produced by *S. aureus* RN6390 *Pspac::sspABC* transformed with pRscpAB, or pRscpA_(C>A)B vector. Cultures were grown in TSB for 6 or 18 h, at which point proteins in the cell free culture supernatant were precipitated with TCA, and subjected to SDS-PAGE. Protein equivalent to 1.0 OD₆₀₀ unit of culture was applied to each lane. The arrow on the third lane of the gel points to the 40 kDa proScpA_(C>A) protein that is prominent at 6 h, but no longer evident after 18 h.

dase at ANA₂₆ESNS (Fig. 7A), and corresponds to the N-terminal propeptide P1. The 20 kDa component visible after 4 h of growth is the first stable MP1 isoform of MP, processed at VT₂₀₃MPTSQF. The middle component evident only after 6 h results from processing of MP1 at FK₂₁₀SNNYT, yielding the MP2 isoform of ScpA (Fig. 6A). Transformation of RN6390 *Pspac::sspABC* with pRscpA_(C>A)B, harbouring a Cys>Ala active site substitution of the ScpA domain, led to accumulation of 40 kDa proScpA after 6 h (Fig. 7C), and several minor polypeptides in the 20 kDa range, which did not match in pattern or abundance with P1, MP1 or MP2. After 18 h, proScpA_(C>A) was no longer evident, but there was no accumulation of the P1-MP1-MP2 triplet. Taken together, these data indicate that proScpA undergoes rapid autocatalytic activation, but is degraded if this is not correctly initiated.

The P1-MP1-MP2 triplet is preceded by a slightly larger isoform (Fig. 7B and inset) that was most evident from 4 to 6 h. Several observations identify this is a transient

MP1' isoform, processed at LE₁₇₆DKKLLK. First, if production of MP1 by processing at VT₂₀₃MPTSQF was the first event in proScpA activation, it would yield a 20.2 kDa P1 fragment extending from Glu₂₆ to Thr₂₀₂, instead of the observed 17 kDa P1. Second, from analysis of column fractions obtained during purification of mature ScpA by cation exchange chromatography (Fig. 8), the C-terminus of P1 was deduced to be Glu₁₇₆, as follows. The MP2 isoform of mature ScpA eluted as a broad peak, where the tail fractions (lanes 1–4) overlapped with a peak containing P1 (lanes 2–5), followed by a sharp peak (lanes 7 and 8) with no protease activity, designated P1'. The N-terminus of P1' results from processing of P1 at IK₃₃AKDKK (Fig. 7A), and mass analysis identified three isoforms in this fraction (Table 4). The major isoform (*m/z* 16573.30) corresponded to P1', extending from Ala₃₃ to Glu₁₇₆. A less abundant isoform is a variant of P1', extending from Ala₃₃ to a secondary processing site at LK₁₇₁. A third isoform (*m/z* of 17346.64) corresponds to overlap from the preceding P1 peak, extending from Glu₂₆ to the

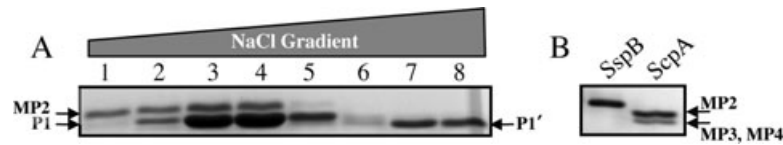


Fig. 8. SDS-PAGE of consecutive fractions eluted in a NaCl gradient, during cation exchange chromatography of culture supernatant protein from *S. aureus* RN6390 *Pspac::sspABC* transformed with *pRscpAB*. Lanes 1 through 4 comprise the tail fractions of a broad peak containing mature ScpA (MP2), which overlaps with a well-defined peak (lanes 2–5) comprised of the 17 P1 propeptide. Lanes 7 and 8 represent late-eluting peak fractions that contain a variant P1' isoform of the propeptide. Fractions from the broad MP2 peak that preceded the trailing fractions shown in lanes 1 and 2 were pooled and concentrated, and shown in (B), compared with purified SspB protease. The identity of the individual polypeptides is as indicated in Fig. 7A.

terminal LE₁₇₆↓ processing site. Therefore, the transient MP1' isoform results from processing at LE₁₇₆↓, which is as an early event in activation of proScpA.

Structural comparisons

To better understand the rapid autocatalytic activation of proScpA, the automated Swiss-Model program (Arnold *et al.*, 2006) was used for structure-based protein alignment and modelling. The best fit for proScpA was with the structure of proSspB, with an excellent overall fit supported by a composite QMEAN score of -74.198 (Benkert *et al.*, 2009), and a DFire (all-atom distance-dependent statistical potential) energy score of -469.37 (Zhou and Zhou, 2002). The ProQRes score that provides a per-residue estimate of model accuracy over a sliding window of nine amino acids (Wallner and Elofsson, 2006) dropped below 0.5 at just three segments. One segment comprises the N-terminus of the MP2 isoform after processing of MP1 at FK₂₁₀↓ *SNNYT* (Fig. 7A). The other segments, which also define sites of autocatalytic processing, are shaded grey in a structure-based alignment to an amino acid sequence that spans the C-terminus of the N-terminal propeptide of proSspB (Fig. 9A). This segment of proSspB is comprised of a β -strand ₁₇₁KVRLVKA₁₇₇, followed by a long unstructured segment, a short helix and another short β -strand (Fig. 9A). These features are coloured magenta in the proSspB structure (Fig. 9B), where the N-terminal propeptide (red) forms a half-barrel with an open interior that is occupied by insertion of a Staphopain-specific loop from the protease domain (blue) (Filipek *et al.*, 2004). The roof of the interior cavity forms a

three-stranded anti-parallel β -sheet, where the third strand (magenta) marks the beginning of the sequence shown in Fig. 9A. The sequence ₁₇₇KATPLAN₁₈₃, spanning the end of this third β -strand and start of the long unstructured segment (Fig. 9A), traverses the active site, blocking access to one side of the catalytic cysteine (Fig. 9B, and enlarged view in C).

The equivalent unstructured segment of proScpA is longer, due to two segments with low ProQRes scores, which do not superimpose over proSspB (Fig. 9A and D). The first of these, *EDKCLK* defines the initial site of autocatalytic processing at LE₁₇₆↓ *DKCLK* (Fig. 7A and B). The second, *GNNVTQLK*↓*QK*, precedes the site that was processed in the cytoplasm of *E. coli*, leading to capture of the MP'' activation intermediate in complex with ScpB (Figs 6A and 7A). Focusing on the first processing site, Leu₁₇₅ is directly above the catalytic cysteine (Fig. 9E), while the preceding Arg₁₇₄ extends towards the cocatalytic His₃₃₄, and is in proximity to Trp₃₅₇, the position of which is conserved in proSspB. Significantly, Arg₁₇₄ in proScpA occupies the same position as Leu₁₈₁ in proSspB, where the position of the inhibitory segment of the propeptide may be stabilized by hydrophobic interaction between Leu₁₈₁ and neighbouring Trp₃₆₂. Potentially, this segment of proScpA is destabilized by placement of the positively charged side-chain of Arg₁₇₄ adjacent to the basic catalytic His₃₃₄, and hydrophobic Trp₃₅₇. Therefore, several factors likely account for the rapid autocatalytic activation of proScpA, which relative to proSspB include: (i) placement of the LE₁₇₆ motif for initial autocatalytic processing directly above the catalytic cysteine, (ii) a longer unstructured segment that traverses the active site, within which

Table 4. Mass spectrum data of purified propeptide fragment, derived from protein shown in Fig. 8, lanes 7 and 8.

Composition ^a (NH ₂ -/-COOH)	Isoform	<i>m/z</i>		Peak area	
		Theoretical	Measured	Absolute	Relative
<u>33AKKDKK</u> -/-LKT ¹⁷⁶ PRLE	P1'	16572.97	16573.30	4284078	100
<u>33AKKDKK</u> -/-NHHKAKLK ¹⁷¹		15976.61	15777.14	1052951	25
<u>26ESNSN</u> -/-LKT ¹⁷⁶ PRLE	P1	17345.99	17346.64	263782	6

a. Experimentally determined N-terminal sequences are underlined, followed by amino acid sequences representing the expected C-terminus, based on the measured *m/z*-values.

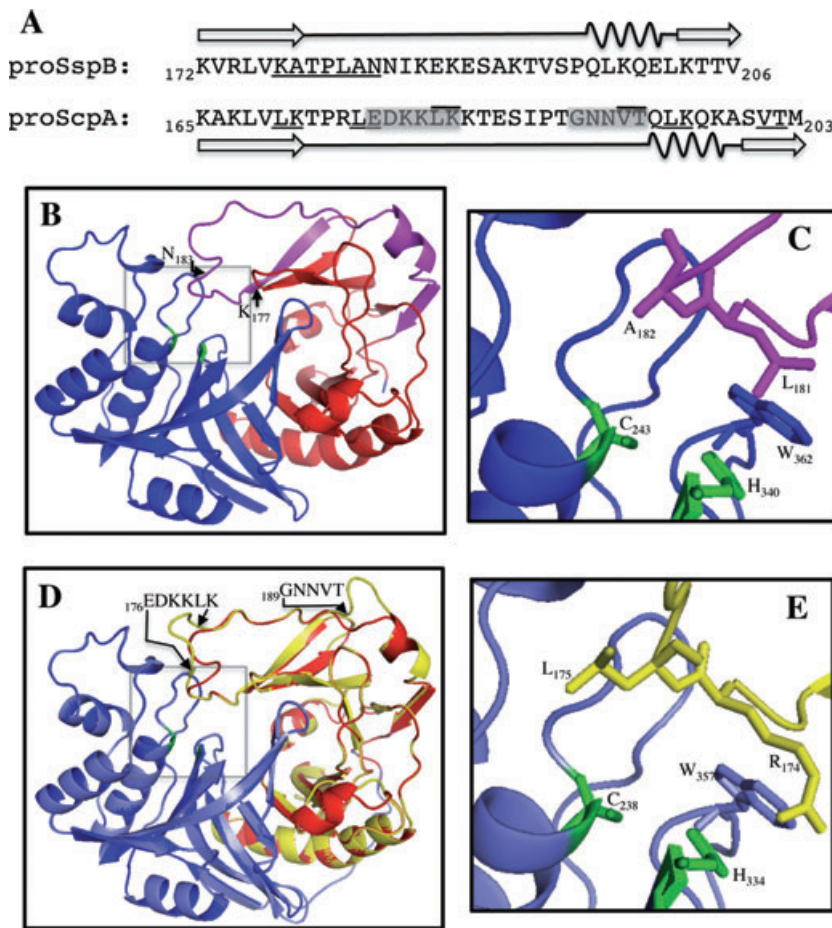


Fig. 9. (A) Amino acid sequence and secondary structure elements spanning the C-terminus of the N-terminal propeptide domain of proSspB (upper), and structure-based alignment to the comparable propeptide segment of proScpA (lower). The underlined motifs in proScpA correspond to processing sites that give rise to the MP1', MP1'' and MP1 isoforms (Fig. 7A), and the overlined motifs represent additional potential processing sites. Grey-shaded sections represent segments with low ProQRes scores, which do not superimpose on the known structure of proSspB, illustrated by arrows in (D). The underlined proSspB segment $_{177}\text{KATPLAN}_{183}$ is critical to maintaining latency of proSspB, as shown in the crystal structure (B), where it blocks access to the active site, shown in enlarged view in (C). The mature SspB domain is dark blue, and the propeptide is red, except for the magenta segment spanning the C-terminus of the propeptide as illustrated in (A). The catalytic Cys $_{243}$ and His $_{340}$ are coloured green, shown in stick configuration in (C). (D) shows a model proScpA structure (ScpA domain is light blue and the propeptide domain is yellow) superimposed on proSspB, shaded dark blue and red as in (B). Arrows point to sections of a long unstructured loop that deviate from the proSspB structure, indicated by grey shading in (A). (E) shows an enlargement of the active site of proScpA, revealing that Leu $_{175}$ in the LE $_{176}\downarrow$ motif that is processed as the initial event in autocatalytic activation, is directly above the catalytic Cys $_{238}$. Additional details are provided in the text.

there are several sites for autocatalytic processing; and (iii) a potential destabilizing effect of Arg $_{174}$ on the inhibitory function of the propeptide.

The same activation intermediates are evident in clinical isolates that express ScpA and degrade elastin

Others described a cysteine protease of *S. aureus* that exhibited elastase activity and processed a synthetic substrate Phe-Leu-Glu-pNA (Potempa *et al.*, 1988). No N-terminal sequence was provided, but the activity on Phe-Leu-Glu-pNA suggested that it could be ScpA, which was also active on this substrate, and processed at LE \downarrow DKK to initiate autocatalytic activation. Elastase activity of ScpA was confirmed by culturing RN6390 *Pspac::sspABC* harbouring pRscpAB on elastin agar, which led to clearing of the elastin fibres (Fig. 10A), while cells harbouring pRscpA $_{(C>A)}$ B had no activity. Screening of additional selected strains (Fig. 10A and B) revealed that RN6390 had no activity, even though it expresses the Aureolysin, SspA and SspB proteases that comprise the SPC pathway (Rice *et al.*, 2001; Nickerson *et al.*, 2007; 2008). Strains Newman and the USA300 and USA400

strains of community-acquired MRSA also had no activity, even though the latter two exhibit *in vitro* expression of proteases of the SPC pathway (Burlak *et al.*, 2007). However, strains belonging to the CC30 clonal complex (Table 1) cleared the elastin, including: (i) WBG10049, which was highly active and corresponds to a hypervirulent community-acquired MRSA (Robinson *et al.*, 2005), (ii) BK12003, a closely related but methicillin susceptible clinical isolate, (iii) M1015, which is a hypervirulent historical pandemic strain (Robinson *et al.*, 2005) and (iv) MN8, which is a prototypic toxic shock syndrome isolate (Blomster-Hautamaa and Schlievert, 1988), and had weaker activity. Strain WBG10049 and additional CC30 clinical isolates were cultured in TSB for 6 or 18 h, followed by trichloroacetic acid (TCA) precipitation of secreted proteins, and SDS-PAGE (Fig. 10C). Each had a cluster of polypeptides similar to those associated with autocatalytic activation of ScpA, and the identity of the P1 polypeptide was confirmed by mass spectrometry for WBG10049 and L516. Therefore, the same activation mechanism for proScpA is observed in clinical isolates belonging to the CC30 clonal complex, and ScpA uniquely confers elastinolytic activity.

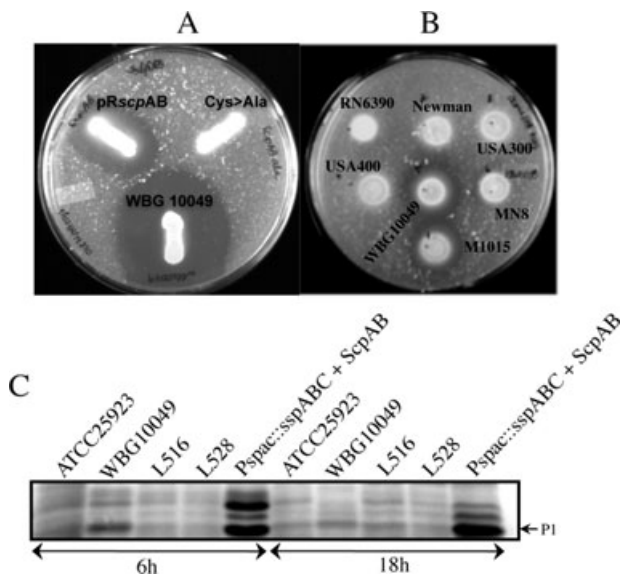


Fig. 10. A and B. Growth on elastin agar of *S. aureus* RN6390 *Pspac::sspABC* harbouring pRscpAB or pRscpA_{(C>A)B} and additional selected strains as indicated. C. Section of SDS-PAGE protein gel showing that polypeptides associated with activation of proScpA are produced by strain WBG10049 and additional related *S. aureus* isolates belonging to clonal complex CC30, as labelled above each lane. Cultures were grown in TSB for 6 or 18 h as indicated, using RN6390 *Pspac::sspABC* harbouring pRscpAB as a reference. The 17 kDa P1 polypeptide band for WBG10049 and L516 were confirmed as the N-terminal propeptide of proScpA by in-gel trypsin digestion and mass spectrometry.

Differential stabilities and substrate specificities of Staphopains A and B

The processing sites identified in association with activation of proScpA (IK↓; LK↓; FK↓; LE↓; VT↓; YT↓; YN↓) are consistent with proteases of the papain family preferring a hydrophobic or bulky aromatic amino acid in the P2 position of the peptide substrate, but generally being less restricted at P1. This broad specificity appears to render ScpA susceptible to autolytic degradation, because it disappeared during extended incubation at 37°C (Fig. 11), but was stabilized by a cysteine-protease inhibitor E64. In contrast, SspB which has a strong preference for Arg in the P1 position (Massimi *et al.*, 2002) was stable under the same conditions. These findings suggest that the broad specificity of ScpA contributes to instability of both the precursor and mature isoforms, but promotes its ability to degrade elastin, in contrast to SspB that has a restricted specificity and is stable in both isoforms, but cannot degrade elastin.

Discussion

We have completed a comparison of the requirement for Staphostatins ScpB and SspC, in relation to the activation

mechanisms and biochemical traits of the Staphopain A (ScpA) and B (SspB) cysteine proteases. Activation of proSspB is the end-point of the SPC, differentiating the proteolytic capacity of *S. aureus* from the CNS represented by *S. epidermidis*. Consequently, the *sspBC* genes are proposed to have evolved in *S. aureus* as paralogues of the ancestral *scpAB* (Golonka *et al.*, 2004; Dubin *et al.*, 2007), which are common to *S. aureus* and CNS. Paralogues by definition should have altered functions relative to their ancestral genes, consistent with our comparison of Staphopains A and B, which are structurally very similar, but differ greatly in their biochemical traits and interaction with cognate Staphostatins. Our work has defined multiple control points in the SPC pathway, which minimize the susceptibility of proSspB to premature activation during protein export. A potentially novel control point is inherent in the cellular retention of preproSspB, which once secreted, is exceptionally sensitive to activation by SspA (Massimi *et al.*, 2002). Conversely, preproSspA is rapidly secreted, but undergoes a slow multistep activation procedure where the final Aureolysin-dependent processing is rate-limiting (Nickerson *et al.*, 2007). The slow secretion of preproSspB and slow activation of proSspA would minimize the probability of preproSspB undergoing premature activation during protein export. Moreover, proSspB appears to be structurally optimized for activation by SspA, because it was stable and unprocessed when secreted into the periplasm of *E. coli*, or when retained in the cytoplasm. This would facilitate the observed cellular retention, which is unlikely to have evolved if preproSspB were prone to premature activation.

The stability of proSspB and its inability to undergo autocatalytic activation likely account for preproSspB being secreted without detriment in the absence of Staphostatin SspC, in contrast to the severe phenotype of a *sspC::tet* insertion mutation in *S. aureus* 8325-4 (Shaw *et al.*, 2005). It is possible that the severity of the *sspC::tet* phenotype was influenced by an adventitious small colony variant (SCV) phenotype that frequently arises in *S. aureus* on exposure to antibiotics, and shares many of the traits of the *sspC::tet* mutant, including slow growth, reduced production of secreted proteins, altered cell-wall

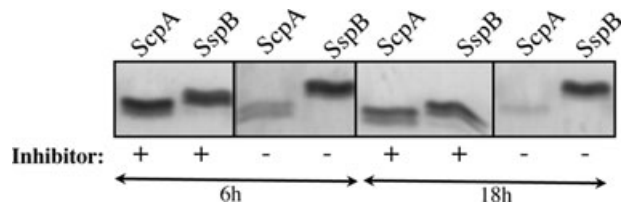


Fig. 11. SDS-PAGE and protein stain of mature ScpA or SspB after incubation for 6 or 18 h in the presence (+) or absence (-) of the cysteine protease specific inhibitor E64, as indicated.

morphology and resistance to lysostaphin and phage-mediated cell lysis (Proctor *et al.*, 2006). SCV isolates are auxotrophic for haemin and menadione, which can rescue the SCV phenotype, and are abundant in BHI but not in TSB (McNamara and Proctor, 2000), consistent with the *sspC::tet* phenotype also being more severe in TSB relative to BHI (Shaw *et al.*, 2005). SCV isolates from human infections uniformly have defects in *menB* (Lannergard *et al.*, 2008), which is required for menadione synthesis, and the entire *menB* gene that is adjacent to the *sspABC* operon was included on the vector used to construct *sspC::tet* (Shaw *et al.*, 2005).

In contrast to proSspB that is optimized for stability, proScpA is optimized for rapid autocatalytic activation, and even with a Cys>Ala active site substitution, was processed in the cytoplasm of *E. coli* to release its N-terminal propeptide. Moreover, autocatalytic activation was initiated when native proScpA was retained in the cytoplasm of *E. coli*, leading to capture by Staphostatin A of the MP1'' activation intermediate, processed several amino acids prior to the N-terminus of mature MP2 isoform. Because Staphostatins are less able to complex with their target Staphopain if the active site cysteine is blocked or modified (Filipek *et al.*, 2003; 2005; Rzychon *et al.*, 2003), the MP1'' isoform is likely the first intermediate where the active site is not obstructed by a residual propeptide segment. Therefore, Staphostatin A functioned as designed and proposed (Potempa *et al.*, 2005; Shaw *et al.*, 2005), to capture an early activation intermediate.

The initial autocatalytic processing at LE₁₇₆↓DK is followed by at least three additional processing events at LK₁₉₆, VT₂₀₂ and FK₂₀₉. The N-terminal propeptide was also processed at IK₃₂ and LK₁₇₁. Therefore, ScpA favours substrates with lysine in the P1 position, but is not restricted to this specificity because other sites were also processed (LE, VT, YT and YN). This activation mechanism and specificity most closely resemble the Streptococcal pyrogenic exotoxin B, SpeB (Streptopain) that accumulates an inactive precursor proSpeB in the culture supernatant during growth of *S. pyogenes* (Liu and Elliott, 1965), followed by autocatalytic intermolecular activation, whereby newly generated mature SpeB activates remaining proSpeB (Doran *et al.*, 1999; Chen *et al.*, 2003). Sites processed during activation of proSpeB included three IK↓ motifs, although other sites were also cleaved, including VN↓ and YA↓ (Doran *et al.*, 1999). Thus, ScpA and SpeB are papain-like cysteine proteases that prefer, but are not restricted to lysine in the P1 position of substrate proteins. Unlike proSpeB, which could also be activated by trypsin, activation of proScpA appears to be primarily intramolecular, such that if self-processing at LE₁₇₆↓DKK does not occur, it is prone to degradation. We cannot completely exclude intermolecular processing by other proteases, because a proScpA_(C>A) isoform was pro-

cessed in the cytoplasm of *E. coli* to release the N-terminal propeptide (Fig. 5). However, proScpA_(C>A) was unstable when secreted by *S. aureus* (Fig. 7C), resembling the Aureolysin metalloprotease, which also underwent rapid intramolecular autocatalytic activation, while an active site substitution derivative was rapidly degraded (Nickerson *et al.*, 2008). Therefore, rapid intramolecular autocatalytic activation appears to occur at the expense of an unstable precursor, which for proScpA is balanced by the protective function of Staphostatin ScpB.

Significantly, the *speB* gene is coexpressed with an adjacent gene encoding a cognate inhibitor designated Spi, which structurally resembles the N-terminal propeptide of proSpeB (Kagawa *et al.*, 2005). As such, the model of Staphostatin function overlooks a fundamental principle of protease precursor activation, whereby the N-terminal propeptide functions both as an intramolecular inhibitor to maintain latency of the precursor during protein export, and as a chaperone to ensure proper folding of the protease domain (Kessler and Safrin, 1994; McIver *et al.*, 1995; Fu *et al.*, 2000; Yabuta *et al.*, 2001). This dual role is normally sufficient to facilitate activation of a protease, while avoiding harm to the cells that produce it. Several studies have confirmed that in the absence of an N-terminal propeptide chaperone, mature but denatured proteases can refold to a near-native conformation, but cannot become active in the absence of the N-terminal propeptide chaperone function (Fu *et al.*, 2000; Yabuta *et al.*, 2001; Jaswal *et al.*, 2002; Jaswal *et al.*, 2005). The SpeB–Spi interaction is an interesting example, where it is pertinent to query whether Spi has maximized inhibitory function while minimizing chaperone function, or if both activities are maintained.

In this context, secretion of microbial proteases may pose unique challenges to the secretion apparatus, because the SecYEG translocon prefers unfolded protein substrates. Opposing this requirement, the N-terminal propeptide of a protease functions as an intramolecular chaperone to promote tight folding of the protease domain, characterized by reduced conformational mobility and high energy barrier to unfolding, conferring stability to the secreted protease in extreme environments, which may include exposure to other proteases (Jaswal *et al.*, 2002; Jaswal *et al.*, 2005). The nature of this dilemma is likely reflected in the diversity of solutions employed by bacteria to secrete proteases. A serine protease of *Aeromonas hydrophila* is expressed without a propeptide, but is coexpressed with an adjacent gene encoding a 13.7 kDa protein, which is secreted into the periplasm and promotes folding of the protease through an intermolecular mechanism (Nomura *et al.*, 2002). Alternately, some extracellular metalloproteases of Gram-negative bacteria are expressed in operons that encode a dedicated secre-

tion apparatus, in addition to a specific inhibitor, the necessity of which has not yet been addressed (Guzzo *et al.*, 1991; Feltzer *et al.*, 2000).

Our data allude to a chaperone function for SspC, because it formed a complex with proSspB when the two proteins were coexpressed in the cytoplasm of *E. coli*. Such an interaction was thought to be unlikely based on their lack of interaction when mixed in solution, consistent with the absence of compatible interfaces that would promote docking interactions (Filipek *et al.*, 2004). An important distinction is that in this study, the complex was captured in the cytoplasm using proSspB that lacked a signal peptide, and only a portion of the total proSspB produced was captured in complex with SspC. Potentially, preproSspB is partially folded in the cytoplasm of *S. aureus*, accounting for the slow secretion, and SspC captures only a fraction of preproSspB that has unfolded to separate the propeptide and protease domains. Alternately, SspC interacts with nascent preproSspB through an as yet unknown specificity, to aid in maintaining secretion competence, thus duplicating the role of the N-terminal propeptide as both an inhibitor and a chaperone. For microbial proteases that are coexpressed with accessory proteins, our study emphasizes that each example must be studied on a case-by-case basis to draw meaningful conclusions, and the possibility of a dual function should be considered.

Relevant to chaperone requirements, our data indicate that proScpA and proSspB have different folding properties, as evident from proScpA(C>A) being captured in complex with the ATP-dependent cytoplasmic chaperone GroEL, which is a homo-oligomer of 14 subunits arranged in two heptameric rings, forming a large central cavity where folding of newly synthesized or transiently unfolded protein takes place (Horwich *et al.*, 2006). In *E. coli*, GroEL also participates in the SecB-dependent secretory pathway, in concert with the molecular chaperones DnaK-DnaJ-GrpE, to maintain proteins in an unfolded conformation compatible with translocation across the cytoplasmic membrane (Phillips and Silhavy, 1990; Wild *et al.*, 1996). Because Gram-positives do not have an equivalent to SecB (van Wely *et al.*, 2001), and proScpA was expressed in *E. coli* without its signal peptide, we cannot comment on the relevance of this interaction to protein secretion. However, we take this as evidence of the different physical properties of proScpA compared with proSspB, and it is feasible that Staphopains A and B have different chaperone requirements and interactions for protein secretion, as suggested by the cellular retention of preproSspB.

Cellular retention could be due to slow translocation across the cytoplasmic membrane, or alternately being efficiently translocated, but slowly processed by signal peptidase. In *Bacillus subtilis*, levansucrase also accumu-

lated with an unprocessed signal peptide, whereas α -amylase was rapidly secreted (Petit-Glatron *et al.*, 1987; Leloup *et al.*, 1997). This was attributed in part to the affinities of the precursors for SecA, the ATPase that interacts with the SecYEG translocase, and it was proposed that α -amylase was less affected by a decrease in SecA, because it has at least an order of magnitude greater affinity for SecA (Leloup *et al.*, 1999). Therefore, slow secretion of preproSspB could be due to a reduced affinity for the Sec machinery, or due to it being partially folded in the cytoplasm, making it a less efficient substrate for the SecYEG translocase. Another bottleneck in secretion is the release from the cell of a precursor isoform whose signal peptide has been cleaved (Leloup *et al.*, 1997; 1999). This was described as a calcium-dependent process that could be influenced by the cell wall, with the unfolded–folded transition being monitored by resistance to proteolysis. Consequently, it is expected that newly translocated but unfolded precursors with unprocessed signal peptides should be sensitive to proteolysis, which is not what we observed for preproSspB, so we favour an explanation whereby translocation is rate-limiting.

It is also important to consider the location of protein secretion. Studies with *S. pyogenes* revealed that the SpeB cysteine protease is secreted through a microdomain of the cellular membrane that is specialized to contain a high concentration of the Sec translocons and accessory factors, adjacent to where the new cell division septum will be formed (Rosch and Caparon, 2004; Rosch and Caparon, 2005). Other studies suggest that this may be a default pathway, evident from the observation that many cell surface proteins in both *S. aureus* and *S. pyogenes* have a YSIRK sorting motif in their signal peptides that dictates trafficking to the septum of the dividing cell, while some cell-surface proteins and most secreted toxins and enzymes that lack this sorting motif will by default be secreted through specific microdomains distributed around the cell (Carlsson *et al.*, 2006; DeDent *et al.*, 2007; 2008). Given that secreted enzymes are maximally expressed by *S. aureus* at high levels in the post-exponential phase of growth, but must traffic through a limited number of microdomains, the retention of preproSspB may be another layer of control that evolved with the SPC pathway to minimize the interaction between protease precursors during protein export, and this will be the focus of future work.

Experimental procedures

Bacterial strains, plasmids and growth conditions

Bacterial strains and plasmids used or created in this study are listed in Tables 1 and 2. Unless otherwise indicated, cultures were grown at 37°C in tryptic soy (Becton Dickinson and Company) for *S. aureus*, and Luria–Bertani broth (Invit-

rogen) respectively. Media were supplemented with agar (15 g l⁻¹), ampicillin (100 µg ml⁻¹), erythromycin (10 µg ml⁻¹) or chloramphenicol (10 µg ml⁻¹) as required. When required for experimental analyses, *S. aureus* were cultured in Erlenmeyer flasks, maintaining a 5:1 ratio of flask to medium volume to ensure proper aeration, and grown with orbital shaking (150 r.p.m.) for the indicated periods of time. *E. coli* DH5α was used for cloning and vector construction, XL-1 Blue was used for site-directed mutagenesis, and M15[pRep] was used for expression of recombinant 6His-tagged proteins.

Plasmid construction

The *S. aureus* and *E. coli* cells were electroporated with a Bio-Rad GenePulser apparatus. Electrocompetent *S. aureus* cells were prepared by washing in ice cold sucrose (Novick, 1991). *S. aureus* genomic DNA was isolated using the DNeasy Tissue Kit (Qiagen) following the manufacturer's protocol for Gram-positive bacteria, incorporating a lysostaphin (50 µg ml⁻¹; Sigma) lysis step. Plasmid DNA was isolated using GenElute Plasmid Mini prep Kit (Sigma) following recommended protocols. Polymerase chain reaction was performed with Biotools DNA polymerase (Interscience) or with Expand Long Template PCR system (Roche Applied Science) for products larger than 2 kb. PCR products were purified using QIAquick PCR Purification Kit (Qiagen). Use of T4 DNA Ligase (New England BioLabs) and Calf Intestine Alkaline Phosphatase (Roche Applied Science) was in accordance with manufacturer's recommendations.

Plasmids defined in Table 2 were created by PCR amplification of segments of genomic or plasmid DNA using primers in Table 3, followed by cloning into the appropriate sites of the vector using restriction sites incorporated into the PCR primers. A Cys>Ala active site substitution in ScpA was obtained by PCR-directed mutagenesis of pUscpAB (Table 2) with primers MP_scpA1 and MP_scpA2 (Table 3), using the QuikChange II-E Site-Directed Mutagenesis Kit (Stratagene), used as described previously (Nickerson *et al.*, 2007; 2008). Mutagenized plasmids were transformed into *E. coli* XL1-Blue for screening purposes, and all plasmids constructed in this study were submitted for verification of nucleotide sequence at the Toronto Center for Applied Genomics facility.

Construction of RN6390_Pspac::sspC and Pspac::sspABC strains

For the RN6390 Pspac::sspC ectopic expression mutant, pMUT_BC was constructed in *E. coli* (Tables 2 and 3), and the suicide vector was electroporated into the RN4220 host strain of *S. aureus*, followed by selection of plasmid integrants on BHI agar supplemented with 10 µg ml⁻¹ Erm. Genomic DNA was extracted from Erm^r transformants, and subjected to PCR with primers sspB_F4 and Mut_R2 to amplify a DNA segment spanning the expected boundary at the 5' end of the integrated plasmid and genomic DNA, while the expected 3' boundary was confirmed with primers Mut_F2 and sspC_R3. Additional details are provided in the results section. Using phage φ85, a lysate was prepared from a transformant that yielded the expected PCR products with

these two primer pairs, and the Pspac::sspC allele was transferred into RN6390 by phage transduction (Novick, 1991).

To construct RN6390 Pspac::sspABC, pMUTIN4 was modified by replacing lacZ with the E194ts temperature-sensitive Gram-positive replication origin (pMUT_E194ts; Table 2). A 346 bp PCR product beginning with the ribosome binding site of sspA was generated by PCR with sspA_F1 and sspA_R1 (Table 3), and cloned into the HindIII and BamHI sites of pMUT_E194ts, adjacent to the IPTG-inducible Pspac promoter. The pMUT_sspA vector was transferred into *S. aureus* RN6390 via the intermediate host RN4220, and once the presence of pMUT_sspA was confirmed by growth at permissive temperature, the vector was integrated into the chromosome by growth at non-permissive temperature, to create RN6390 Pspac::sspABC, where the sspABC operon is disrupted by integration of pMUT_sspA at the 5' end of sspA.

Cellular fractionation and protein localization

For fractionation experiments, *S. aureus* cells were grown for 6 h in TSB, then mixed with an equal volume of ice cold 50 mM sodium azide and 200 µM CCCP (carbonyl cyanide m-chlorophenylhydrazone; Sigma), and immediately centrifuged at 2000 g for 20 min at 4°C. Cell pellets were washed in 1× SMM (0.5 M sucrose, 15 mM sodium maleate, 20 mM MgCl₂) and resuspended in 1× SMM to achieve a cell density of 10¹⁰ cfu ml⁻¹. Lysostaphin was added (10 µg ml⁻¹) and incubated 15 min at 37°C. Spheroplast formation was confirmed by mixing a drop of the suspension on a glass slide with a drop of 1% SDS. Subsequently, an aliquot of sample was removed and boiled in 1% SDS to prepare total cell lysate. The remaining sample was centrifuged at 1900 g for 15 min, and the supernatant was collected, representing cell surface proteins. The spheroplast pellet was washed once in 1× SMM, and resuspended in the same volume of 1× SDS-PAGE sample buffer. After boiling to promote lysis, this fraction comprised the combined membrane and cytoplasmic proteins. Where indicated, a washed cell suspension of 10¹⁰ cfu ml⁻¹ was treated with 10 µg ml⁻¹ proteinase K or buffer alone for 30 min at 37°C, followed by addition of 1 mM Pefabloc (Roche Applied Science) and extensive washing, prior to preparation of total cell lysate.

The *E. coli* cultures for protein localization were grown 5 h in 2YT media. Cultures were centrifuged and cells were resuspended in 50 mM sodium phosphate buffer, pH 7.4, 140 mM NaCl and 20 mg ml⁻¹ polymyxin B sulphate (8100 USP units mg⁻¹; Sigma). Polymyxin B treatment was for 20 min on ice with gentle shaking, followed by centrifugation at 16 000 g for 10 min at 4°C. The supernatant fraction represents periplasmic proteins, and the cell pellet constitutes cytoplasmic and membrane proteins (Zollman *et al.*, 1994).

Protein expression and purification

Proteins were purified with an AKTA FPLC system (Amersham Biosciences). For purification of mature ScpA, *S. aureus* RN6390 Pspac::sspABC harbouring pRscpAB was grown for 6 h in TSB. Cells were removed by centrifugation, and after supplementing the cell-free culture supernatant with 1 mM EDTA, proteins were precipitated by addition of 80%

saturation of ammonium sulphate, then dissolved and dialysed into 20 mM sodium phosphate, pH 7.4. Protein was filtered through a 0.20 µm filter before application to a HiTrap SP HP ion exchange column (Amersham Biosciences). Bound proteins were eluted over a linear NaCl gradient up to 1.0 M NaCl in 50 mM sodium phosphate, at a flow rate of 2 ml min⁻¹, while collecting 2 ml fractions. Column fractions were assessed by SDS-PAGE and assay with Phe-Leu-Glu-pNA substrate. Fractions active on Phe-Leu-Glu-pNA were enriched in a 20 kDa protein, and those exhibiting the least amount of other contaminating proteins were pooled and subjected to size exclusion chromatography on HiLoad 16/60 Superdex 75 column.

For expression and purification of 6His-tagged proteins in *E. coli* M15[pREP], gene expression was induced with 1 mM IPTG for 4 h. Subsequent preparation of cell lysate and purification of recombinant proteins by MAC using a HiTrap HP Chelating affinity column (Amersham Biosciences) was performed as described previously (Nickerson *et al.*, 2007; 2008). Similar protocols were followed for expression and purification of 6His-tagged proteins that were expressed from the pBAD24 vector in *E. coli* DH10B, except that expression was induced with 0.02% arabinose. Protein concentrations were determined using the bicinchoninic acid protein assay reagent (Pierce).

Enzyme and elastin-agar assays

ScpA protease activity was measured by monitoring the release of p-nitroaniline (pNA) from chromogenic substrate Z-Phe-Leu-Glu-pNA (Bachem). Assays were conducted in triplicate wells of a microtiter plate in a 100 µl volume containing 100 mM sodium phosphate, pH 7.4, 2 mM cysteine, 5 mM EDTA and 0.4 mM substrate. Absorbances were measured on a microplate reader (BioTek) with a 405 nm filter. Elastin degradation was by growth on elastin agar (per litre; 15 g agar, 3 g elastin bovine neck ligament, 2.5 g yeast extract, 1.0 g glucose, 4.41 g hydrated trisodium citrate, 1.0 g sodium caseinate) supplemented with 2 mM cysteine and 20 mM CaCl₂. For each *S. aureus* strain to be tested, 5 µl of an exponential phase culture grown in TSB was spotted onto the elastin agar, and allowed to grow for 4 days at 37°C, after which zones of elastin clearing could be visualized.

Protein modelling

The amino acid sequence of the proScpA protein encoded by SAOUHSC_02127 of *S. aureus* strain 8325-4 was submitted to the automated Swiss-Model server (Arnold *et al.*, 2006), to produce a model proScpA structure superimposed on the known structure of proSspB (Filipek *et al.*, 2004). The quality of the model was assessed using protein structure and model assessment programmes provided by Swiss-Model, include QMEAN and DFire that provide pseudo energy values as an estimation of the overall model structural accuracy (Zhou and Zhou, 2002; Benkert *et al.*, 2009), and ProQRes that provides a measure of the local quality of the model over a moving window of nine amino acids (Wallner and Elofsson, 2006).

Antibody production

Recombinant SspC_6H was purified by MAC of cell lysate from *E. coli* transformed with pBAD_{sspC_6H} as previously described (Massimi *et al.*, 2002). Purified protein (100 µg) was emulsified in Freund's complete adjuvant (Sigma) and injected subcutaneously into each of two New Zealand White rabbits with booster injections administered at 2 week intervals, consisting of 100 µg protein emulsified in Freund's incomplete adjuvant (Sigma). Antibodies were affinity purified from antisera obtained after the second boost, using recombinant SspC_6H and reagents and protocols provided with the AminoLink Plus Immobilization Kit (Pierce). Similar procedures were followed to obtain affinity purified antibodies specific for SspA and proSspB as described previously (Nickerson *et al.*, 2007; 2008). The purified antibodies were used in Western blot assays at 5000× dilution.

SDS-PAGE, Western blotting and N-terminal sequencing

Cell-free culture supernatant was precipitated with an equal volume of ice cold 20% (w/v) TCA. Cell lysates were prepared by incubating washed cells with 25 µg ml⁻¹ lysostaphin for 30 min at 37°C, followed by boiling with 1% SDS for 5 min. TCA-precipitated samples and cell lysates were subjected to SDS-PAGE and visualized by staining with Coomassie brilliant blue R-250. For Western blotting, proteins were transferred to PVDF membrane (Millipore), which were processed for Western blot analysis, including blocking and incubation with primary and secondary antibody (AffiniPure goat anti-rabbit IgG; Jackson Immuno Research Laboratories) as described previously (Nickerson *et al.*, 2007), and Hla-specific antibodies were purchased from Sigma. Blots were developed with 5-bromo-4-chloro-3-indolylphosphate and nitroblue tetrazolium alkaline phosphate substrates (Bio-Rad).

For N-terminal sequence determination, proteins were separated by SDS-PAGE and transferred to PVDF membrane using CAPS transfer buffer (Yuen *et al.*, 1989). Protein bands were visualized by staining with 0.1% Coomassie Blue in 40% methanol, excised with a scalpel and submitted to the Advanced Protein Technology Center at the Hospital for Sick Children for N-terminal sequence determination.

Mass spectrometry

Coomassie-Blue stained protein bands from SDS-PAGE were excised and digested with trypsin (Promega) using an in-gel digestion protocol. Samples were submitted to the Proteomics Core Facility of the Toronto Angiogenesis Research Center at Sunnybrook Health Sciences Centre. Peptides were analysed by LC-MS/MS using the Agilent 1100 nanoflow HPLC with Agilent XCT-Plus ion trap (Agilent Technologies), and the database search against NCBI nr was performed by Spectrum Mill software (Agilent Technologies). For mass determination, purified proteins were exchanged into 5% formic acid by ultrafiltration, then diluted 20-fold in 50% acetonitrile and 2% formic acid, and analysed by ESI-QqTOF (QStar-XL, Applied Biosystems/MDS Sciex) through infusion

at 6 $\mu\text{l min}^{-1}$ flow rate. The machine was cleaned by infusing 100 μl of 50% trifluoroethanol to eliminate carryover between samples, and calibrated immediately before each sample. Spectra accumulated over 3 min of steady spray were used for molecular weight reconstruction with 'Bayesian Protein Reconstruct' in the BioAnalyst 1.1.5 software package (Applied Biosystems/MDS Sciex) using default settings.

Acknowledgements

This work was supported by CIHR Operating Grant MOP-12669 to M.J.M. N.N. was the recipient of a University of Toronto Open Fellowship Award. We thank Latha Jacob and Carly Pigeon for technical assistance, and Eric Yang for expert assistance with mass spectrometry, through the Proteomics Core Facility of the Toronto Angiogenesis Research Centre.

References

- Archer, G.L. (1998) *Staphylococcus aureus*: a well-armed pathogen. *Clin Infect Dis* **26**: 1179–1181.
- Arnold, K., Bordoli, L., Kopp, J., and Schwede, T. (2006) The SWISS-MODEL workspace: a web-based environment for protein structure homology modelling. *Bioinformatics* **22**: 195–201.
- Baba, T., Takeuchi, F., Kuroda, M., Yuzawa, H., Aoki, K., Oguchi, A., *et al.* (2002) Genome and virulence determinants of high virulence community-acquired MRSA. *Lancet* **359**: 1819–1827.
- Baba, T., Bae, T., Schneewind, O., Takeuchi, F., and Hiramatsu, K. (2008) Genome sequence of *Staphylococcus aureus* strain Newman and comparative analysis of Staphylococcal genomes: polymorphism and evolution of two major pathogenicity islands. *J Bacteriol* **190**: 300–310.
- Benkert, P., Kunzli, M., and Schwede, T. (2009) QMEAN server for protein model quality estimation. *Nucleic Acids Res* **37**: W510–W514.
- Blomster-Hautamaa, D.A., and Schlievert, P.M. (1988) Preparation of toxic shock syndrome toxin-1. *Methods Enzymol* **165**: 37–43.
- Bubeck Wardenburg, J., Bae, T., Otto, M., Deleo, F.R., and Schneewind, O. (2007) Poring over pores: alpha-hemolysin and Panton-Valentine leukocidin in *Staphylococcus aureus* pneumonia. *Nat Med* **13**: 1405–1406.
- Burlak, C., Hammer, C.H., Robinson, M.A., Whitney, A.R., McGavin, M.J., Kreiswirth, B.N., and Deleo, F.R. (2007) Global analysis of community-associated methicillin-resistant *Staphylococcus aureus* exoproteins reveals molecules produced *in vitro* and during infection. *Cell Microbiol* **9**: 1172–1190.
- Carlsson, F., Stalhammar-Carlemalm, M., Flardh, K., Sandin, C., Carlemalm, E., and Lindahl, G. (2006) Signal sequence directs localized secretion of bacterial surface proteins. *Nature* **442**: 943–946.
- Chen, C.Y., Luo, S.C., Kuo, C.F., Lin, Y.S., Wu, J.J., Lin, M.T., *et al.* (2003) Maturation processing and characterization of Streptopain. *J Biol Chem* **278**: 17336–17343.
- DeDent, A.C., McAdow, M., and Schneewind, O. (2007) Distribution of Protein A on the surface of *Staphylococcus aureus*. *J Bacteriol* **189**: 4473–4484.
- DeDent, A., Bae, T., Missiakas, D.M., and Schneewind, O. (2008) Signal peptides direct surface proteins to two distinct envelope locations of *Staphylococcus aureus*. *EMBO J* **27**: 2656–2668.
- Doran, J.D., Nomizu, M., Takebe, S., Menard, R., Griffith, D., and Ziomek, E. (1999) Autocatalytic processing of the Streptococcal cysteine protease zymogen: processing mechanism and characterization of the autoproteolytic cleavage sites. *Eur J Biochem* **263**: 145–151.
- Dubin, G., Wladyka, B., Stec-Niemczyk, J., Chmiel, D., Zdzalik, M., Dubin, A., and Potempa, J. (2007) The Staphostatin family of cysteine protease inhibitors in the genus *Staphylococcus* as an example of parallel evolution of protease and inhibitor specificity. *Biol Chem* **388**: 227–235.
- Feltzer, R.E., Gray, R.D., Dean, W.L., and Pierce, W.M., Jr (2000) Alkaline proteinase inhibitor of *Pseudomonas aeruginosa*. Interaction of native and N-terminally truncated inhibitor proteins with *Pseudomonas* metalloproteinases. *J Biol Chem* **275**: 21002–21009.
- Filipek, R., Rzychon, M., Oleksy, A., Gruca, M., Dubin, A., Potempa, J., and Bochtler, M. (2003) The Staphostatin-Staphopain complex: a forward binding inhibitor in complex with its target cysteine protease. *J Biol Chem* **278**: 40959–40966.
- Filipek, R., Szczepanowski, R., Sabat, A., Potempa, J., and Bochtler, M. (2004) Prostaphopain B structure: a comparison of proregion-mediated and Staphostatin-mediated protease inhibition. *Biochemistry* **43**: 14306–14315.
- Filipek, R., Potempa, J., and Bochtler, M. (2005) A comparison of Staphostatin B with standard mechanism serine protease inhibitors. *J Biol Chem* **280**: 14669–14674.
- Fowler, V.G., Jr, Nelson, C.L., McIntyre, L.M., Kreiswirth, B.N., Monk, A., Archer, G.L., *et al.* (2007) Potential associations between hematogenous complications and bacterial genotype in *Staphylococcus aureus* infection. *J Infect Dis* **196**: 738–747.
- Fu, X., Inouye, M., and Shinde, U. (2000) Folding pathway mediated by an intramolecular chaperone. The inhibitory and chaperone functions of the Subtilisin propeptide are not obligatorily linked. *J Biol Chem* **275**: 16871–16878.
- Golonka, E., Filipek, R., Sabat, A., Sinczak, A., and Potempa, J. (2004) Genetic characterization of Staphopain genes in *Staphylococcus aureus*. *Biol Chem* **385**: 1059–1067.
- Guzman, L.M., Belin, D., Carson, M.J., and Beckwith, J. (1995) Tight regulation, modulation, and high-level expression by vectors containing the arabinose pBAD promoter. *J Bacteriol* **177**: 4121–4130.
- Guzzo, J., Duong, F., Wandersman, C., Murgier, M., and Lazdunski, A. (1991) The secretion genes of *Pseudomonas aeruginosa* alkaline protease are functionally related to those of *Erwinia chrysanthemi* proteases and *Escherichia coli* alpha-hemolysin. *Mol Microbiol* **5**: 447–453.
- Hofmann, B., Schomburg, D., and Hecht, H.J. (1993) Crystal structure of a thiol protease proteinase from *Staphylococcus aureus* V-8 in the E-64 inhibitor complex. *Acta Crystallogr* **A49** (Suppl): 102.
- Horwich, A.L., Farr, G.W., and Fenton, W.A. (2006) GroEL-GroES-mediated protein folding. *Chem Rev* **106**: 1917–1930.
- Jaswal, S.S., Sohl, J.L., Davis, J.H., and Agard, D.A. (2002)

- Energetic landscape of alpha-lytic protease optimizes longevity through kinetic stability. *Nature* **415**: 343–346.
- Jaswal, S.S., Truhlar, S.M., Dill, K.A., and Agard, D.A. (2005) Comprehensive analysis of protein folding activation thermodynamics reveals a universal behavior violated by kinetically stable proteases. *J Mol Biol* **347**: 355–366.
- Kagawa, T.F., O'Toole, P.W., and Cooney, J.C. (2005) SpeB-Spi: a novel protease-inhibitor pair from *Streptococcus pyogenes*. *Mol Microbiol* **57**: 650–666.
- Kessler, E., and Saffrin, M. (1994) The propeptide of *Pseudomonas aeruginosa* elastase acts an elastase inhibitor. *J Biol Chem* **269**: 22726–22731.
- Lannergard, J., von Eiff, C., Sander, G., Cordes, T., Seggewiss, J., Peters, G., et al. (2008) Identification of the genetic basis for clinical menadione-auxotrophic small-colony variant isolates of *Staphylococcus aureus*. *Antimicrob Agents Chemother* **52**: 4017–4022.
- Leloup, L., Haddaoui el, A., Chambert, R., and Petit-Glatron, M.F. (1997) Characterization of the rate-limiting step of the secretion of *Bacillus subtilis* alpha-amylase overproduced during the exponential phase of growth. *Microbiology* **143**: 3295–3303.
- Leloup, L., Le Saux, J., Petit-Glatron, M.F., and Chambert, R. (1999) Kinetics of the secretion of *Bacillus subtilis* levanase overproduced during the exponential phase of growth. *Microbiology* **145**: 613–619.
- Li, M., Diep, B.A., Villaruz, A.E., Braughton, K.R., Jiang, X., DeLeo, F.R., et al. (2009) Evolution of virulence in epidemic community-associated methicillin-resistant *Staphylococcus aureus*. *Proc Natl Acad Sci USA* **106**: 5883–5888.
- Liu, T.Y., and Elliott, S.D. (1965) Streptococcal Proteinase: the zymogen to enzyme transformation. *J Biol Chem* **240**: 1138–1142.
- Lowy, F.D. (1998) *Staphylococcus aureus* infections. *N Engl J Med* **339**: 520–532.
- Luchansky, J.B., Benson, A.K., and Atherly, A.G. (1989) Construction, transfer and properties of a novel temperature-sensitive integrable plasmid for genomic analysis of *Staphylococcus aureus*. *Mol Microbiol* **3**: 65–78.
- McGavin, M.J., Zahradka, C., Rice, K., and Scott, J.E. (1997) Modification of the *Staphylococcus aureus* fibronectin binding phenotype by V8 protease. *Infect Immun* **65**: 2621–2628.
- McIver, K.S., Kessler, E., Olson, J.C., and Ohman, D.E. (1995) The elastase propeptide functions as an intramolecular chaperone required for elastase activity and secretion in *Pseudomonas aeruginosa*. *Mol Microbiol* **18**: 877–889.
- McNamara, P.J., and Proctor, R.A. (2000) *Staphylococcus aureus* small colony variants, electron transport and persistent infections. *Int J Antimicrob Agents* **14**: 117–122.
- Massimi, I., Park, E., Rice, K., Muller-Esterl, W., Sauder, D., and McGavin, M.J. (2002) Identification of a novel maturation mechanism and restricted substrate specificity for the SspB cysteine protease of *Staphylococcus aureus*. *J Biol Chem* **277**: 41770–41777.
- Nickerson, N.N., Prasad, L., Jacob, L., Delbaere, L.T., and McGavin, M.J. (2007) Activation of the SspA serine protease zymogen of *Staphylococcus aureus* proceeds through unique variations of a trypsinogen-like mechanism and is dependent on both autocatalytic and metalloprotease-specific processing. *J Biol Chem* **282**: 34129–34138.
- Nickerson, N.N., Joag, V., and McGavin, M.J. (2008) Rapid autocatalytic activation of the M4 metalloprotease aureolysin is controlled by a conserved N-terminal fungalsin-thermolysin-propeptide domain. *Mol Microbiol* **69**: 1530–1543.
- Nomura, T., Fujii, Y., Yamanaka, H., Kobayashi, H., and Okamoto, K. (2002) The protein encoded at the 3' end of the serine protease gene of *Aeromonas sobria* functions as a chaperone in the production of the protease. *J Bacteriol* **184**: 7058–7061.
- Novick, R.P. (1991) Genetic systems in Staphylococci. *Methods Enzymol* **204**: 587–636.
- Patti, J.M., Allen, B.L., McGavin, M.J., and Hook, M. (1994) MSCRAMM-mediated adherence of microorganisms to host tissues. *Annu Rev Microbiol* **48**: 585–617.
- Patti, J.M., and Hook, M. (1994) Microbial adhesins recognizing extracellular matrix macromolecules. *Curr Opin Cell Biol* **6**: 752–758.
- Peng, H.L., Novick, R.P., Kreiswirth, B., Kornblum, J., and Schlievert, P. (1988) Cloning, characterization, and sequencing of an accessory gene regulator (*agr*) in *Staphylococcus aureus*. *J Bacteriol* **170**: 4365–4372.
- Petit-Glatron, M.F., Benyahia, F., and Chambert, R. (1987) Secretion of *Bacillus subtilis* levansucrase: a possible two-step mechanism. *Eur J Biochem* **163**: 379–387.
- Phillips, G.J., and Silhavy, T.J. (1990) Heat-shock proteins DnaK and GroEL facilitate export of LacZ hybrid proteins in *E. coli*. *Nature* **344**: 882–884.
- Potempa, J., Dubin, A., Korzus, G., and Travis, J. (1988) Degradation of elastin by a cysteine proteinase from *Staphylococcus aureus*. *J Biol Chem* **263**: 2664–2667.
- Potempa, J., Golonka, E., Filipek, R., and Shaw, L.N. (2005) Fighting an enemy within: cytoplasmic inhibitors of bacterial cysteine proteases. *Mol Microbiol* **57**: 605–610.
- Proctor, R.A., von Eiff, C., Kahl, B.C., Becker, K., McNamara, P., Herrmann, M., and Peters, G. (2006) Small colony variants: a pathogenic form of bacteria that facilitates persistent and recurrent infections. *Nat Rev Microbiol* **4**: 295–305.
- Rice, K., Peralta, R., Bast, D., de Azavedo, J., and McGavin, M.J. (2001) Description of staphylococcus serine protease (*ssp*) operon in *Staphylococcus aureus* and nonpolar inactivation of *sspA*-encoded serine protease. *Infect Immun* **69**: 159–169.
- Robinson, D.A., Kearns, A.M., Holmes, A., Morrison, D., Grundmann, G., Edwards, H., et al. (2005) Re-emergence of early pandemic *Staphylococcus aureus* as a community-acquired methicillin-resistant clone. *Lancet* **365**: 1256–1258.
- Rosch, J., and Caparon, M. (2004) A microdomain for protein secretion in Gram-positive bacteria. *Science* **304**: 1513–1515.
- Rosch, J.W., and Caparon, M.G. (2005) The ExPortal: an organelle dedicated to the biogenesis of secreted proteins in *Streptococcus pyogenes*. *Mol Microbiol* **58**: 959–968.
- Rzychon, M., Sabat, A., Kosowska, K., Potempa, J., and Dubin, A. (2003) Staphostatins: an expanding new group of proteinase inhibitors with a unique specificity for the regulation of Staphopains, *Staphylococcus spp.* cysteine proteinases. *Mol Microbiol* **49**: 1051–1066.

- Shaw, L.N., Golonka, E., Szmyd, G., Foster, S.J., Travis, J., and Potempa, J. (2005) Cytoplasmic control of premature activation of a secreted protease zymogen: deletion of Staphostatin B (SspC) in *Staphylococcus aureus* 8325-4 yields a profound pleiotropic phenotype. *J Bacteriol* **187**: 1751–1762.
- Vagner, V., Dervyn, E., and Ehrlich, S.D. (1998) A vector for systematic gene inactivation in *Bacillus subtilis*. *Microbiology* **144**: 3097–3104.
- Wallner, B., and Elofsson, A. (2006) Identification of correct regions in protein models using structural, alignment, and consensus information. *Protein Sci* **15**: 900–913.
- Wardenburg, J.B., and Schneewind, O. (2008) Vaccine protection against *Staphylococcus aureus* pneumonia. *J Exp Med* **205**: 287–294.
- van Wely, K.H., Swaving, J., Freudl, R., and Driessen, A.J. (2001) Translocation of proteins across the cell envelope of Gram-positive bacteria. *FEMS Microbiol Rev* **25**: 437–454.
- Wild, J., Rossmeyssl, P., Walter, W.A., and Gross, C.A. (1996) Involvement of the DnaK-DnaJ-GrpE chaperone team in protein secretion in *Escherichia coli*. *J Bacteriol* **178**: 3608–3613.
- Wladyka, B., Puzia, K., and Dubin, A. (2005) Efficient co-expression of a recombinant Staphopain A and its inhibitor Staphostatin A in *Escherichia coli*. *Biochem J* **385**: 181–187.
- Yabuta, Y., Takagi, H., Inouye, M., and Shinde, U. (2001) Folding pathway mediated by an intramolecular chaperone: propeptide release modulates activation precision of pro-subtilisin. *J Biol Chem* **276**: 44427–44434.
- Yokoi, K., Kakikawa, M., Kimoto, H., Watanabe, K., Yasukawa, H., Yamakawa, A., *et al.* (2001) Genetic and biochemical characterization of glutamyl endopeptidase of *Staphylococcus warneri* M. *Gene* **281**: 115–122.
- Yuen, S.W., Chui, A.H., Wilson, K.J., and Yuan, P.M. (1989) Microanalysis of SDS-PAGE electroblotted proteins. *Bio-techniques* **7**: 74–83.
- Zhou, H., and Zhou, Y. (2002) Distance-scaled, finite ideal-gas reference state improves structure-derived potentials of mean force for structure selection and stability prediction. *Protein Sci* **11**: 2714–2726.
- Zollman, T.M., Austin, P.R., Jablonski, P.E., and Hovde, C.J. (1994) Purification of recombinant Shiga-like toxin type I, A1 fragment from *Escherichia coli*. *Protein Expr Purif* **5**: 291–295.